Chapter 4

Modulating nAChR Agonist Specificity by Computational Protein Design

4.1 INTRODUCTION

Ligand gated ion channels (LGIC) are transmembrane proteins involved in biological signaling pathways. These receptors are therapeutic targets for Alzheimer's, Schizophrenia, drug addiction, and learning and memory.[1,2] LGICs are one type of receptor that binds the neurotransmitter and undergoes a conformational change to allow the passage of ions through the otherwise impermeable cell membrane. A number of studies have identified key interactions that lead to binding of small molecules at the agonist-binding site of LGICs. High-resolution structural data on neuroreceptors are only just becoming available,[3-5] and functional data are still needed to further understand the binding and subsequent conformational changes that occur during channel gating.

Nicotinic acetylcholine receptors (nAChR) are the most extensively studied members of the Cys-loop family of LGICs. The embryonic mouse muscle nAChR is a transmembrane protein composed of five subunits, $(\alpha_1)_2\beta_1\gamma\delta$. Biochemical studies [6,7] and the crystal structure of the acetylcholine-binding protein (AChBP),[3] a soluble protein highly homologous to the ligand-binding domain of the nAChR (**Figure 4.1**), identified two agonist-binding sites at the α/γ and α/δ interfaces on the muscle-type nAChR that are defined by a box of conserved aromatic amino acid residues. The principal face of the agonist-binding site contains four of the five conserved aromatic box residues, while the complementary face contains the remaining aromatic residue.

Structurally similar nAChR agonists acetylcholine, nicotine, and epibatidine (**Figure 4.2**) bind to the same aromatic-binding site with differing activity. Recently, Sixma and co-workers published a nicotine-bound crystal structure of AChBP[4] which reveals additional agonist-binding determinants. To verify the functional importance of potential

agonist-receptor interactions revealed by the AChBP structures, chemical-scale investigations have been performed to identify mechanistically significant drug-receptor interactions at the muscle-type nAChR.[8,9] These studies identified subtle differences in the binding determinants that differentiate ACh, nicotine, and epibatidine activity.

```
AChBP-L         LDRADILYN-IRQTSR----PDVIPTQRDR-PVAVSVSLKFINILEVNEITNEVDVVFWQ
AChBP-A         --QANLMRLKSDLFNR----SPMYPGPTKDDPLTVTLGFTLQDIVKVDSSTNEVDLVYYE
alpha-m         LGSEHETRLVAKLFED--YSSVVRPVEDHREIVQVTVGLQLIQLINVDEVNQIVTTNVRL
beta-m          RGSEAEGQLIKKLFSN--YDSSVRPAREVGDRVGVSIGLTLAQLISLNEKDEEMSTKVYL
gamma-m         QSRNQEERLLADLMRN--YDPHLRPAERDSDVVNVSLKLTLTNLISLNEREEALTTNVWI
delta-m         WGLNEEQRLIQHLFNEKGYDKDLRPVARKEDKVDVALSLTLSNLISLKEVEETLTTNVWI

AChBP-L         QTTWSDRTLAWNSSHSP--DQVSVPISSLWVPDLAAYNAISKPEVLTPQLARVVS-DGEV
AChBP-A         QQRWKLNSLMWDPNEYGNITDFRTSAADIWTPDITAYSSTRPVQVLSPQIAVVTH-DGSV
alpha-m         KQQWVDYNLKWNPDDYGGVKKIHIPSEKIWRPDVVLYNNADGDFAIVKFTKVLLDYTGHI
beta-m          DLEWTDYRLSWDPAEHDGIDSLRITAESVWLPDVVLLNNNDGNFDVALDINVVVSFEGSV
gamma-m         EMQWCDYRLRWDPKDYEGLWILRVPSTMVWRPDIVLENNVDGVFEVALYCNVLVSPDGCI
delta-m         DHAWVDSRLQWDANDFGNITVLRLPPDMVWLPEIVLENNNDGSFQISYACNVLVYDSGYV
                  57

AChBP-L         LYMPSIRQRFSCDVSGVDTESG-ATCRIKIGSWTHHSREISVDPTTEN----------S
AChBP-A         MFIPAQRLSFMCDPTGVDSEEG-VTCAVKFGSWVYSGFEIDLKTDTDQ----------V
alpha-m         TWTPPAIFKSYCEIIVTHFPFDEQNCSMKLGTWTYDGSVVAINPESDQ--------P--D
beta-m          RWQPPGLYRSSCSIQVTYFPFDWQNCTMVFSSYSYDSSEVSLKTGLDPE---GEERQEVY
gamma-m         YWLPPAIFRSSCSISVTYFPFDWQNCSLIFQSQTYSTSEINLQLSQED----GQAIEWIF
delta-m         TWLPPAIFRSSCPISVTYFPFDWQNCSLKFSSLKYTAKEITLSLKQEEENNRSYPIEWII
                   116

AChBP-L         DDSEYFSQYSRFEILDVTQKKNSVTYSC--C-PEAYEDVEVSLNFRKKGRSEIL------
AChBP-A         DLSSYYAS-SKYEILSATQTRQVQHYSC--C-PEPYIDVNLVVKFRERRAGNGFFRNLFD
alpha-m         LSN--FMESGEWVIKEARGWKHWVFYSC--CPTTPYLDITYHFVMQRLPLYFIVNVIIPC
beta-m          IHEGTFIENGQWEIIHKPSRLIQLPGDQRGGKEGHHEEVIFYLIIRRKPLFYLVNVIAPC
gamma-m         IDPEAFTENGEWAIRHRPAKMLLDSVAP--AEEAGHQKVVFYLLIQRKPLFYVINIIAPC
delta-m         IDPEGFTENGEWEIVHRAAKLNVDPSVP--MDSTNHQDVTFYLIIRRKPLFYIINILVPC
```

Figure 4.1 Sequence Alignment of AChBP with Mouse-Muscle nAChR. AChBP-L (AChBP *Lymnaea*) and AChBP-A (AChBP *Aplysia*) are soluble proteins that bind ACh. The predicted mutations are from design calculations on AChBP-L and nicotine complex. The binding pockets on nAChR mouse muscle are formed between the principle subunit, alpha, and complementary subunits, beta, gamma, and delta. The highly conserved aromatic box residues are highlighted in magenta. Residue positions of the predicted mutations are highlighted in cyan and are indicated with AChBP numbering.

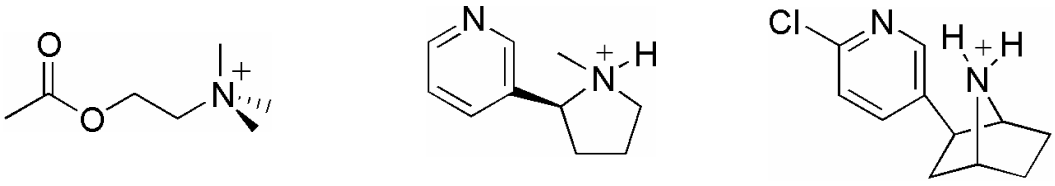

Acetylcholine **Nicotine** **Epibatidine**

Figure 4.2. Structures of nAChR Agonists: acetylcholine, nicotine, and epibatidine**.**

Interestingly, these three agonists also display different relative activity among different nAChR subtypes. For example, the neuronal α7 nAChR subtype displays the following order of agonist potency: epibatidine > nicotine > ACh.[10] For the mouse-muscle subtype the following order of agonist potency is observed: epibatidine>ACh>>nicotine.[8, 11] A better understanding of residue positions that play a role in agonist specificity would provide insight into the conformational changes that are induced upon agonist binding. This information could also aid in designing nAChR sub-type specific drugs.

The present study probes the residue positions that affect nAChR agonist specificity for acetylcholine, nicotine, and epibatidine. To accomplish this goal, we utilized AChBP as a model system for computational protein design studies to improve the poor specificity of nicotine at the muscle-type nAChR.

Computational protein design is a powerful tool for the modification of protein-protein,[12] protein-peptide,[13] and protein-ligand[14] interactions. For example, a designed calmodulin with 13 mutations from the wild-type protein showed a 155-fold increase in binding specificity for a peptide.[13] In addition, Looger et al. engineered proteins from the periplasmic binding protein superfamily to bind trinitrotoluene at nanomolar affinity, and

lactate and serotonin at micromolar affinity.[14] These studies demonstrate the ability of computational protein design to successfully predict mutations that dramatically affect binding specificity of proteins.

With the availability of the 2.2 Å crystal structure of AChBP-nicotine complex,[4] the present study predicted mutations in efforts to stabilize AChBP in the nicotine-preferred conformation by computational protein design. AChBP, although not a functional full-length ion channel, provides a highly homologous model system to the extracellular ligand-binding domain of nAChRs. The present study utilizes mouse-muscle nAChR as the functional receptor to experimentally test the computational predictions. By stabilizing AChBP in the nicotine-bound conformation, we aim to modulate the binding specificity of the highly homologous muscle-type nAChR for three agonists: nicotine, acetylcholine, and epibatidine.

4.2 MATERIALS AND METHODS

Computational Protein Design with ORBIT

The AChBP-nicotine structure (1uwa) was obtained from the Protein Data Bank.[4] The subunits forming the binding site at the interface of B and C were selected for our design, while the remaining three subunits (A, D, E) and the water molecules were deleted. Hydrogens were added with the Reduce program of MolProbity (http://kinemage.biochem.duke.edu/molprobity) and minimized briefly with ORBIT. The ORBIT protein design suite uses a physically based force-field and combinatorial optimization algorithms to determine the optimal amino acid sequence for a protein structure.[15,16] A backbone dependent rotamer library with $\chi 1$ and $\chi 2$ angles expanded by

±15° was used.[17] Charges for nicotine were calculated *ab initio* with Jaguar (Shrodinger) using density field theory with the exchange-correlation hybrid B3LYP and 6-31G** basis set. Nine residues (chain B: 89, 143, 144, 185, 192. chain C: 104, 112, 114, 53) interacting directly with nicotine are considered the primary shell and were allowed to be all amino acids except Gly. Residues contacting the primary shell residues are considered the secondary shell (chain B: 87, 139, 141, 142, 146, 149, 182, 183, 184. chain C: 33, 34, 36, 51, 55, 57, 75, 98, 99, 102, 106, 110, 113, 116). Wild-type Pro and Gly were not designed. 87B, 33C, and 113C were allowed to be all nonpolar amino acids except methionine, and 144B, 146B, 182B, 34C, 57C, 75C, and 116C were allowed to be all polar residues. A tertiary shell includes residues within 4 Å of primary and secondary shell residues, and they were allowed to change in amino acid conformation but not identity. A bias towards the wild-type sequence using the SBIAS module was applied at 1, 2, and 4 kcal*mol^{-1}. An algorithm based on the dead end elimination theorem (DEE) was used to obtain the global minimum energy amino acid sequence and conformation (GMEC).[18]

Mutagenesis and Channel Expression

mRNA was prepared by *in vitro* runoff transcription using the AMbion mMagic mMessage kit. Site-directed mutagenesis was performed using Quick-Change mutagenesis and was verified by sequencing. For nAChR expression, a total of 4.0 ng of mRNA was injected in the subunit ration of 2:1:1:1 for α:β:γ:δ. The β subunit contained a L9'S mutation, as discussed below. Mouse-muscle embryonic nAChR in the pAMV vector was used, as reported below.

Electrophysiology

Stage VI oocytes of *Xenopus laevis* were harvested according to approved procedures. Oocyte recordings were made 24 to 48 h post-injection in two-electrode voltage clamp mode using the OpusXpress^{TM} 600A (Molecular Devices Corporation, Union City, California).[8, 19] To obtain sufficient nicotine signals, oocytes expressing the γ121Qδ123Q mutant were incubated 72 to 96 h post-injection. Oocytes were superfused with calcium-free ND96 solution at flow rates of 1ml/min, 4 ml/min during drug application, and 3 ml/min wash. Cells were voltage clamped at –60 mV. Data were sampled at 125 Hz and filtered at 50 Hz. Drug applications were 15 s in duration. ACh and nicotine were purchased from Sigma/Aldrich/RBI: (-)-nicotine tartrate and acetylcholine chloride. Epibatidine was also purchased from Tocris as (±) epibatidine. All drugs were prepared in calcium-free ND96. Dose-response data were obtained for a minimum of 10 concentrations of agonists and for a minimum of 4 different cells. Curves were fitted to the Hill equation to determine EC_{50} and Hill coefficient.

4.3 RESULTS

Computational Design

The design of AChBP in the nicotine-bound state predicted 10 mutations. To identify those predicted mutations that contribute the most to the stabilization of the structure, we used the SBIAS module of ORBIT, which applies a bias energy toward wild-type residues. We identified two predicted mutations, T57R and S116Q (AChBP numbering will be used unless otherwise stated) in the secondary shell of residues, with strong interaction energies. These residues are on the complementary subunit of the binding

pocket (chain C) and formed inter-subunit side chain to backbone hydrogen bonds to the primary shell residues (**Figure 4.3**). S116Q reaches across the interface to form a hydrogen bond with a donor to acceptor distance of 3.0 Å with the backbone oxygen of Y89, one of the aromatic box residues important in forming the binding pocket. T57R makes a network of hydrogen bonds. E110 flips from the crystallographic conformation to form a hydrogen bond with a donor to acceptor distance of 3.0 Å with T57R, which also hydrogen bonds with E157 in its crystallographic conformation. T57R could also form a potential hydrogen bond, with a donor to acceptor distance of 3.6 Å, to the backbone oxygen of C187, part of a disulfide cysteine bond on a principal loop in the binding domain. Most of the nine primary shell residues kept the crystallographic conformations, a testament to the high affinity of AChBP for nicotine (K_d = 45 nM).[4]

Position 57 is not conserved. From the sequence alignment (**Figure 4.1**) residue 57 is Q, E, Q, A in the alpha, beta, gamma, and delta subunits, respectively. Interestingly, position 57 is naturally R in AChBP from *Aplysia californica*, a different species of snail. Position 116, on the other hand, is highly conserved in nAChRs. In all four mouse muscle nAChR subunits, residue 116 is a P, part of a PP sequence. Study of the 116Q mutant will provide important insight into the necessity of the PP sequence for nAChR function.

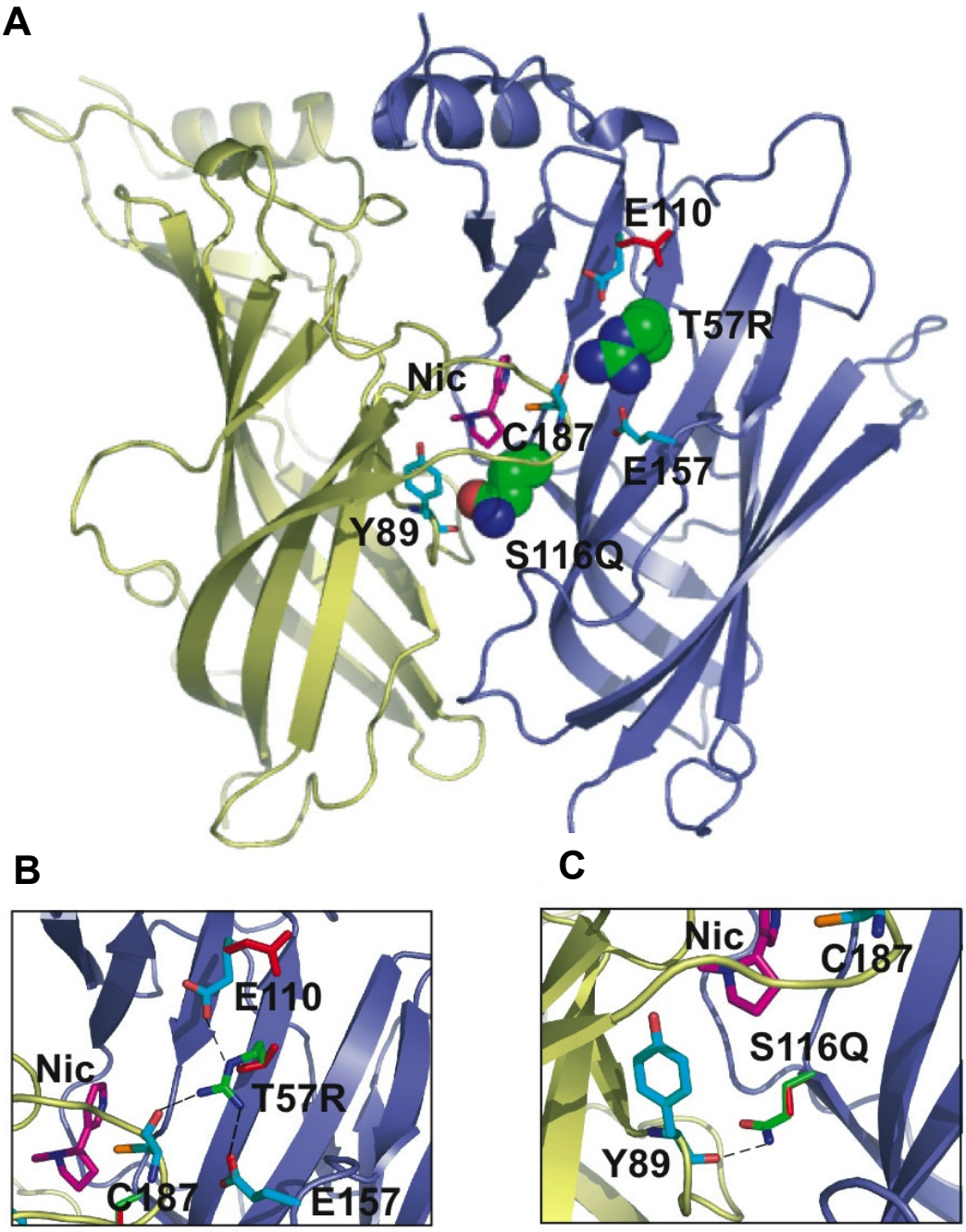

Figure 4.3. Predicted Mutations from Computational Design of AChBP. **A**) Ribbon diagram of two AChBP subunits. Yellow: principle subunit. Blue: complementary subunit. Nicotine, the predicted mutations, and interacting side chains are shown in CPK-inspired colors. Nicotine: magenta. Predicted mutations: green in space-filling model. Interacting residues: cyan. Crystallographic conformations are shown in red. **B**) Close-up view of T57R interactions. **C**) Close-up view of S116Q. Hydrogen bonds are shown as black dashed lines.

Mutagenesis

The following mutations were created on the mouse muscle nAChR: γQ59R, δA61R, γP121Q, and δP123Q. The mutant receptors were evaluated using electrophysiology. When studying weak agonists and/or receptors with diminished binding capability, it is necessary to introduce a Leu-to-Ser mutation at a site known as 9' in the second transmembrane region of the β subunit.[8,9] This 9' site in the β subunit is almost 50 Å from the binding site, and previous work has shown that a L9'S mutation lowers the effective concentration at half maximal response (EC_{50}) by a factor of roughly 40.[9,20] Results from earlier studies[9,20] and data reported below demonstrate that trends in EC_{50} values are not perturbed by L9'S mutations. In addition, the alpha subunits contain an HA epitope between M3-M4. Control experiments show a negligible effect of this epitope tag on EC_{50}.[8] Measurements of EC_{50} represent a functional assay; all mutant receptors reported here are functioning ligand gated ion channels. It should be noted that the EC_{50} value is not a binding constant, but a composite of equilibria for both binding and gating.

Nicotine Specificity Enhanced by 57R Mutation

The ability of the γ59Rδ61R mutant to impact nicotine specificity at the muscle-type nAChR was tested by determining the EC_{50} in the presence of acetylcholine, nicotine, and epibatidine (**Figure 4.4**). The EC_{50} values for the wild-type and mutant receptors are shown in **Table 4.1**. The computational design studies predict this mutation will help stabilize the nicotine-bound conformation by enabling a network of hydrogen bonds with side chains of E110 and E157 as well as the backbone carbonyl oxygen of C187.

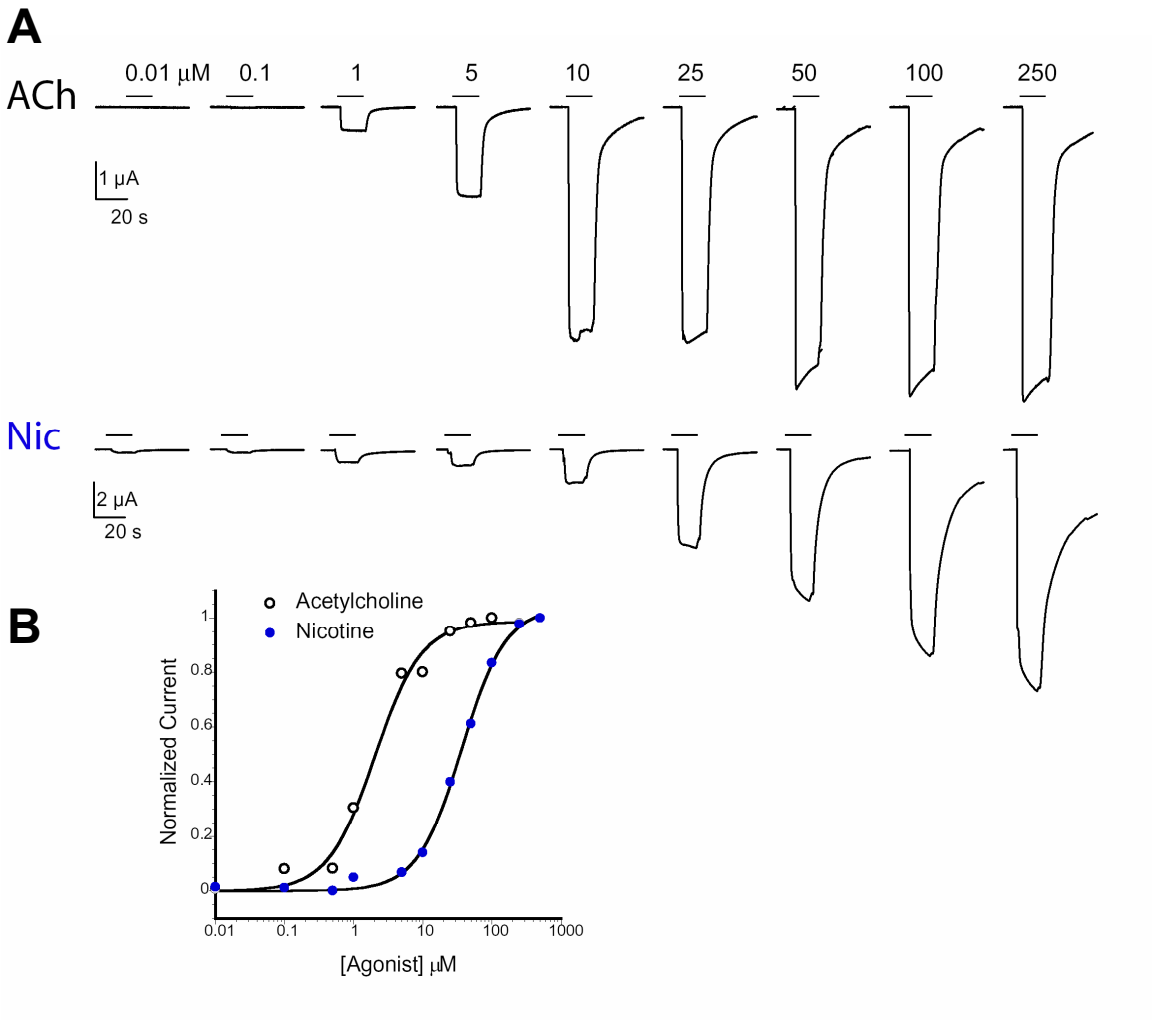

Figure 4.4. Electrophysiology Data. Electrophysiological analysis of ACh and nicotine. **A)** Representative voltage clamp current traces for oocytes expressing mutant muscle nAChRs $(\alpha 1)\beta_9\gamma 59R\delta 61R$. Bars represent application of ACh and nicotine at the concentrations noted. **B**. Representative ACh (o) and nicotine (●) dose-response relations and fits to the Hill equation for oocytes expressing $(\alpha 1)\beta_9\gamma 59R\delta 61R$ nAChRs.

Upon the γ59Rδ61R mutation, the EC_{50} of nicotine *decreases* 1.8-fold compared to the wild-type value, thus improving the potency of nicotine for the muscle-type nAChR. Conversely, ACh shows a 3.9-fold *increase* in EC_{50} compared to the wild-type value, thus decreasing the potency of ACh for the nAChR. The values for epibatidine are relatively unchanged in the presence of the mutation in comparison to wild-type. Interestingly,

these data show a change in agonist specificity of ACh and epibatidine in comparison to nicotine for the nAChR (**Table 4.2)**. The wild-type receptor prefers ACh 69-fold more than nicotine and epibatidine 95-fold more than nicotine. The agonist specificity is significantly changed with the γ59Rδ61R mutant where the receptor's preference for ACh decreases to 10-fold over nicotine. Epibatidine *decreases* to 44-fold over nicotine. The specificity change can be quantified in the ΔΔG values. These values indicate a more favorable interaction for nicotine (-0.3 kcal/mol) than for ACh (0.8 kcal/mol) and epibatidine (0.1 kcal/mol) in the presence of the γ59Rδ61R mutant compared to wild-type receptors.

Table 4.1. EC_{50} Values for Designed nAChR Mutants [a]

Agonist	Wild-type [b]	γ59Rδ61R	γ121Qδ123Q	γ121Q59R-δ123Q61R
ACh	0.83 ± 0.04	3.2 ± 0.4	130 ± 10	180 ± 10
Nicotine	57 ± 2	32 ± 3	180 ± 10	-- [c]
Epibatidine	0.60 ± 0.04	0.72 ± 0.05	45 ± 9	-- [c]

[a] EC_{50} (μM) ± standard error of the mean. (-) Nicotine and racemic epibatidine were used in these experiments. The receptor has a Leu9'Ser mutation in M2 of the β subunit. Mouse muscle nAChR numbering is indicated. [b] Data reported previously.[8] [c] Value difficult to obtain due to insufficient signal.

Table 4.2. Mutations Enhance Nicotine Specificity

Agonist	Wild-type[a] Nic/Agonist	γ59Rδ61R Nic/Agonist	γ121Qδ123Q Nic/Agonist
ACh	69	10	1.4
Nicotine	1	1	1
Epibatidine	95	44	4

Ratio of EC_{50}s for nicotine over indicated agonist (Nic/Agonist). (-) Nicotine and racemic epibatidine were used in these experiments. The receptor has a Leu9'Ser mutation in M2 of the β subunit. Mouse muscle nAChR numbering is indicated. [a] Data reported previously.

Nicotine Specificity Enhanced by 116Q Mutation

The computational design studies predict that the 116Q mutation enables an inter-subunit hydrogen bond with the backbone carbonyl of Y89 and the side chain of 116Q. The impact of the γ121Qδ123Q mutant on channel function at the muscle-type nAChR was tested in the presence of acetylcholine, nicotine, and epibatidine. The EC_{50} values for the wild-type and mutant receptors are show in **Table 4.1**. The EC_{50} of ACh *increases* 160-fold for the γ121Qδ121Q mutant compared to the wild-type value. The mutant results in a 51-fold *increase* in epibatidine EC_{50} compared to the wild-type value. The γ121Qδ121Q mutant, however, results in a smaller 3.2-fold *increase* in nicotine EC_{50}. Interestingly, these data show a more dramatic change in agonist specificity of ACh and epibatidine than observed with the γ59Rδ61R mutation (**Table 4.2)**. The agonist specificity is significantly changed with the γ121Qδ121Q mutant where the receptor's preference for ACh decreases to 1.4-fold over nicotine and for epibatidine *decreases* to 4-fold over nicotine.

Efficacy studies of the γ121Qδ121Q mutant were conducted to determine the relative agonist strength of ACh, nicotine, and epibatidine. Nicotine and epibatidine efficacy, relative to ACh, are extremely low for the γ121Qδ121Q mutant, approximately 2% and 8%, respectively. The efficacy experiments were conducted by applying the following concentrations for each agonist: 500 μM ACh, 750 μM nicotine, and 75 μM epibatidine. Mean whole-cell currents were obtained and normalized to the maximal signal elicited for ACh; ACh is assumed to be a full agonist. Thus, nicotine and epibatidine appear to be partial agonists for the mutant. Overall, the γ121Qδ121Q mutant dramatically impairs agonist activity for ACh, epibatidine, and nicotine. Similarly, receptors containing the double mutation γ121Q59Rδ123Q61R were difficult to monitor in the presence of nicotine and epibatidine due to insufficient signal. It is likely that the γ121Qδ123Q mutant contributes to the impaired channel function for the double mutant. Further studies on this double mutation are necessary to understand the impact of the double mutation.

4.4 DISCUSSION

A better understanding of residue positions that play a role in forming agonist-specific binding sites would provide insight into the nAChR gating mechanism and could also aid in designing nAChR sub-type specific drugs. Because the aromatic box is nearly 100% conserved among nAChRs, we hypothesize that agonist specificity does not depend on the amino acid composition of the binding site itself, but on specific conformations of the aromatic residues. It is possible that the secondary shell residues,

significantly less conserved among nAChR sub-types, play a role in stabilizing unique agonist-preferred conformations of the binding site.

Because the nicotine-bound conformation was used as the basis for the computational design calculations, the design generated mutations that would further stabilize the nicotine-bound state. The 57R mutation, a secondary shell residue on the complementary face of the binding domain, was designed to interact with the primary face shell residue C187 across the subunit interface to stabilize the nicotine-preferred conformation. The 57R mutation electrophysiology data demonstrate an increase in preference in nicotine for the receptor compared to wild-type receptors. The activity of ACh, structurally different from nicotine, decreases, possibly because it undergoes an energetic penalty to re-organize the binding site into an ACh-preferred conformation or to bind to a nicotine-preferred conformation. The change in ACh and nicotine preference for the designed binding pocket conformation leads to a 6.9-fold *increase* in specificity for nicotine in the presence of 57R. The activity of epibatidine, structurally similar to nicotine, remains relatively unchanged in the presence of the 57R mutation. Perhaps the binding site conformation of epibatidine more closely resembles that of nicotine and therefore does not undergo a significant change in activity in the presence of this mutation. Therefore, only a 2.2-fold increase in agonist specificity is observed for nicotine over epibatidine.

The 116Q mutation, also on the complementary face, was designed to create an inter-subunit hydrogen bond between the side chain of 116Q with the backbone carbonyl of the binding-site residue Y89. More dramatic changes in nicotine specificity are observed with the 116Q mutation where a 49-fold *increase* in nicotine specificity relative

to ACh and a 24-fold *increase* in nicotine specificity relative to epibatidine are observed. Thus, position 116 and 57 are important in determining agonist specificity.

Although designed to stabilize the nicotine-bound state, this 116Q mutation dramatically impairs channel function. The γP121QδP121Q mutant results in large EC_{50} values for ACh and epibatidine and poor efficacy for nicotine and epibatidine. It is important to note that the computational design experiments modeled only agonist binding to the ligand-binding domain and cannot account for the impact of these mutations on activity of the full-length channel. In particular, the design is unable to predict the impact of these mutations on channel gating. It is possible that the observed increase in EC_{50}s and decrease in efficacy for the γP121QδP121Q mutant could be attributed partly to impaired channel gating.

These observations for the γP121QδP121Q mutant are consistent with previous studies that examine the impact of a mutation at a homologous site in the ε subunit of adult nAChRs, εP121L.[21,22] This mutation, found in patients with congenital myasthenic syndrome, was shown to dramatically impair channel opening kinetics and to decrease ligand affinity for the open and desensitized nAChR states. Therefore mutation of this highly conserved residue at position 116 to either L or Q dramatically impairs nAChR channel function.

The ability of each single mutation to enhance nicotine specificity of the mouse nAChR demonstrates the importance of the secondary shell residues surrounding the agonist-binding site in determining agonist specificity. In addition, these studies demonstrate a successful application of computational protein design in predicting mutations to enhance ligand specificity. Future studies could include probing the

generality of these observations to other nAChR subtypes and other Cys-loop family members. As additional crystallographic data become available this method could be extended to investigate other ligand-bound LGIC binding sites.

4.5 REFERENCES

1. Paterson, D. & Nordberg, A. Neuronal nicotinic receptors in the human brain. *Progress in Neurobiology* **61**, 75-111 (2000).
2. Cassels, B. K., Bermudez, I., Dajas, F., Abin-Carriquiry, J. A. & Wonnacott, S. From ligand design to therapeutic efficacy: the challenge for nicotinic receptor research. *Drug Discovery Today*, 1657-1665.
3. Brejc, K. et al. Crystal structure of an ACh-binding protein reveals the ligand-binding domain of nicotinic receptors. *Nature* **411**, 269-76 (2001).
4. Celie, P. H. N. et al. Nicotine and Carbamylcholine Binding to Nicotinic Acetylcholine Receptors as Studied in AChBP Crystal Structures. *Neuron* **41**, 907-914 (2004).
5. Unwin, N. Refined structure of the nicotinic acetylcholine receptor at 4A resolution. *Journal of Molecular Biology* **346**, 967-89 (2005).
6. Grutter, T. & Changeux, J. P. Nicotinic receptors in wonderland. *Trends in Biochemical Sciences* **26**, 459-463 (2001).
7. Karlin, A. Emerging structure of the nicotinic acetylcholine receptors. *Nature Reviews Neuroscience* **3**, 102-14 (2002).
8. Cashin, A. L., Petersson, E. J., Lester, H. A. & Dougherty, D. A. Using physical chemistry to differentiate nicotinic from cholinergic agonists at the nicotinic acetylcholine receptor. *Journal of the American Chemical Society* **127**, 350-356 (2005).
9. Beene, D. L. et al. Cation-pi interactions in ligand recognition by serotonergic (5-HT3A) and nicotinic acetylcholine receptors: the anomalous binding properties of nicotine. *Biochemistry* **41**, 10262-9 (2002).
10. Gerzanich, V. et al. Comparative pharmacology of epibatidine: a potent agonist for neuronal nicotinic acetylcholine receptors. *Molecular Pharmacology* **48**, 774-82 (1995).
11. Rush, R., Kuryatov, A., Nelson, M. E. & Lindstrom, J. First and second transmembrane segments of alpha3, alpha4, beta2, and beta4 nicotinic acetylcholine receptor subunits influence the efficacy and potency of nicotine. *Molecular Pharmacology* **61**, 1416-22 (2002).
12. Kortemme, T. et al. Computational redesign of protein-protein interaction specificity. *Nature Structural and Molecular Biology* **11**, 371-9 (2004).
13. Shifman, J. M. & Mayo, S. L. Exploring the origins of binding specificity through the computational redesign of calmodulin. *Proceedings of the National Academy of Sciences U S A* **100**, 13274-9 (2003).
14. Looger, L. L., Dwyer, M. A., Smith, J. J. & Hellinga, H. W. Computational design of receptor and sensor proteins with novel functions. *Nature* **423**, 185-90 (2003).
15. Dahiyat, B. I. & Mayo, S. L. De novo protein design: fully automated sequence selection. *Science* **278**, 82-7 (1997).
16. Mayo, S. L., Olafson, B. D. & Goddard, W. A. Dreiding-a Generic Force-Field for Molecular Simulations. *Journal of Physical Chemistry* **94**, 8897-8909 (1990).
17. Dunbrack, R. L., Jr. & Cohen, F. E. Bayesian statistical analysis of protein side-chain rotamer preferences. *Protein Science* **6**, 1661-81 (1997).

18. Pierce, N. A., Spriet, J. A., Desmet, J. & Mayo, S. L. Conformational splitting: A more powerful criterion for dead-end elimination. *Journal of Computational Chemistry* **21**, 999-1009 (2000).
19. Lummis, S. C. et al. Cis-trans isomerization at a proline opens the pore of a neurotransmitter-gated ion channel. *Nature* **438**, 248-52 (2005).
20. Kearney, P. C. et al. Agonist binding site of the nicotinic acetylcholine receptor: Tests with novel side chains and with several agonists. *Molecular Pharmacology* **50**, 1401-1412 (1996).
21. Sine, S. M. et al. Naturally Occurring Mutations at the Acetylcholine Receptor Binding Site Independently Alter ACh Binding and Channel Gating. *The Journal of General Physiology* **120**, 483-496 (2002).
22. Ohno, K. et al. Congenital myasthenic syndrome caused by decreased agonist binding affinity due to a mutation in the acetylcholine receptor epsilon subunit. *Neuron* **17**, 157-70 (1996).